ORGANIC LETTERS

2004
Vol. 6, No. 2
189−192

Origin of Stereochemical Reversal in Meyers-Type Enolate Alkylations. Importance of Intramolecular Li Coordination and Solvent Effects

Yasuhiro Ikuta and Shuji Tomoda*

Department of Life Sciences, Graduate School of Arts and Sciences, The University of Tokyo, Komaba, Meguro-ku, Tokyo 153-8902, Japan

tomoda@selen.c.u-tokyo.ac.jp

Received October 16, 2003

ABSTRACT

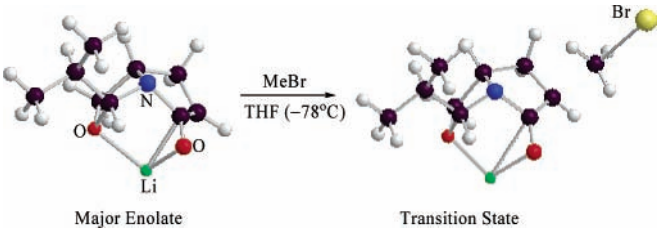

The origin of exclusive *exo*-stereochemistry in the alkylation of Meyers-type enolate 2 has been studied. It was found that the intramolecular complex with a strong Li···O(ring) interaction (the O-complex) may be responsible as the major enolate species in tetrahydrofuran (THF). The transition state of the O-complex leading to *exo*-stereochemistry is found to be the most favorable process in THF.

Over the years much effort has been devoted to search the origin of π-facial diastereoselection.[1] Recently it was shown[2] that there is no theoretical ground in the mutually opposite assertions of the two conventional transition state models (Felkin−Anh model[3] and Cieplak model[4]), both of which focus on the antiperiplanar hyperconjugative stabilization effect involving the incipient (forming) bond as the origin of facial diastereoselection. The debate in this area has been brought up to a new stage.[5] An investigation of well-known controversial cases, in which elaborate experimental data are available, may offer a clue to shed new light on this historical topic in organic chemistry.

Perhaps the most intriguing but puzzling case is nearly complete stereochemical reversal in alkylations of Meyers-type lactam enolates, Li-enolates **1** (*endo*-selective) and **2** (*exo*-selective), where the only structural difference is the position of the oxygen atom in the oxazolidine ring adjacent to the lactam enolate moiety.[6]

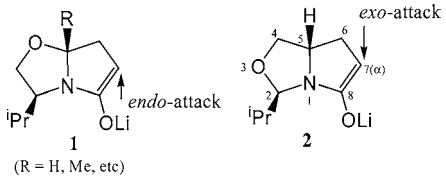

In a recent communication,[7] we reported that exceedingly high stereoselectivity (99%) in the alkylation of 1,5-dim-

(1) For a recent review on this subject, see: le Noble, W. J.; Gung, B. W. Ed. *Chem. Rev.* **1999**, *99*, 1069. Special issue on diastereoselection.

(2) (a) Kaneno, D.; Tomoda, S. *Org. Lett.* **2003**, *5*, 2947. (b) Tomoda, S. *Chem. Rev.* **1999**, *99*, 1243. (c) Tomoda, S.; Senju, T. *Tetrahedron* **1999**, *55*, 5303. (d) Tomoda, S.; Senju, T. *Chem. Commun.* **1998**, 423. (e) Tomoda, S.; Senju, T. *Tetrahedron* **1999**, *55*, 3871. (f) Tomoda, S.; Kaneno, D.; Senju, T. *Heterocycles* **2000**, *50*, 1435. (g) Tomoda, S.; Zhang, J.; Kaneno, D.; Segi, M.; Zhou, A. *Tetrahedron. Lett.* **2000**, *41*, 4597. (h) Butkus, E.; Stoncius, A.; Mallinauskiene, J.; Tomoda, S.; Kaneno, D. *Can. J. Chem.* **2001**, *79*, 1598.

(3) Anh, N. T. *Top. Curr. Chem.* **1980**, *88*, 145.

(4) Cieplak, A. S. *J. Am. Chem. Soc.* **1981**, *103*, 4540.

(5) (a) Knoll, W.; Bobeck, M. M.; Kalchhauser, H.; Rosenberg, M. G.; Brinker, U. H. *Org. Lett.* **2003**, *5*, 2943. (b) Smith, R. J.; Trzoss, M.; Bühl, M.; Bienz, S. *Eur. J. Org. Chem.* **2002**, 2770. (c) Luibrand, R. T.; Taigounov, I. R.; Taigounov, A. A. *J. Org. Chem.* **2001**, *66*, 7254. (d) Rosenberg, R. E.; Abel, R. L.; Drake, M. D.; Fox, D. J.; Ignatz, A. K.; Kwait, D. M.; Schaal, K. M.; Virker, P. R. *J. Org. Chem.* **2001**, *66*, 1694.

10.1021/ol036021q CCC: $27.50
Published on Web 12/31/2003

ethylpyrrolidin-2-one Li-enolate (**3**), a model compound for **1**,[8] was ascribed to the high predominance of the Li species, in which Li coordinates the enolate C═C π-bond from the *endo*-face, both in the gas phase and in tetrahydrofuran (THF). An alkyl halide preferentially attacks at the enolate α-carbon (C3 in **3**) from the sterically favorable *endo*-face, where HOMO is much more expanded. It was suggested that significant pyramidalization at C3 by strong Li coordination should be responsible for nearly complete *endo*-attack. In the present study similar analysis has been applied to the unusual behavior of bicyclic lactam enolate **2**. The results of computational studies are described herein.[9−11]

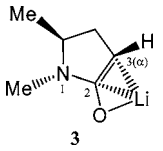

3

One could reasonably assume that the unique stereochemical reversal between enolates **1** and **2** might arise from 1,2-transposition of the oxygen atom in the oxazolidine ring. A molecular model shows that the ring oxygen atom can come quite close to the Li atom within the concavity of the conformationally flexible bicyclic system of **2**. It was therefore expected that in addition to the previously identified four enolate types (**C**-*endo*, **C**-*exo*, **N**, and **F**),[12] a novel enolate species with an intramolecular O−Li···O interaction (denoted as **O**) may be present in solution (THF) (Scheme 1) and that this one might be responsible for nearly exclusive *exo*-selectivity. Structure optimization at the B3LYP/6-31G-(d) level indicated that among the five possible enolate species, the free Li enolate (**F**) was converted into **N** species upon repeated trials of geometry optimization.

Scheme 1. Possible Enolate Species of **2**[12]

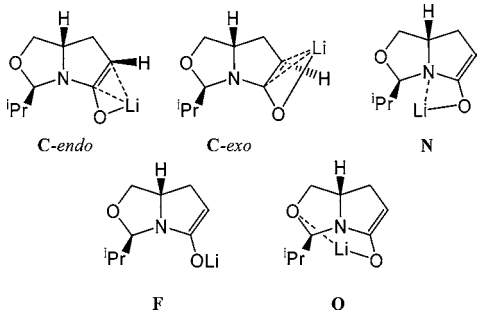

Table 1. Thermodynamic Stability of Possible Enolates (**2**) in the Gas Phase and in Tetrahydrofuran (THF)

	gas phase[b]		THF[c]	
enolates (**1**)[a]	rel E[d] (kcal/mol)	population[e] (%)	rel E[d] (kcal/mol)	population[e] (%)
C-*endo*	1.81	0.9	0.63	16.4
C-*exo*	4.06	0.0	4.09	0.0
N	4.08	0.0	1.91	0.6
O	0.00	99.1	0.00	83.0

[a] See text, ref 12, and Scheme 1 for enolate notations and structures. [b] B3LYP/6-31G(d)// B3LYP/6-31G(d). [c] THF = tetrahydrofuran (dielectric constant = 7.52); B3LYP/6-311+G(d,p)//B3LYP/6-31G(d) using the CPCM method.[9,11] [d] Energy relative to the most stable enolate species (**O**). [e] Relative abundance calculated at 195.15 K (−78 °C).

Table 1 shows the relative stability of the four remaining enolate species (**C**-*endo*, **C**-*exo*, **N**, and **O**). Indeed the **O**-complex enolate (**O**) is major both in the gas phase (99.1%) and in THF solution (83.0%). It should be noted that **C**-*exo*, which should undergo preferential *exo*-alkylation with an alkyl halide according to the conclusion from the previous work,[7,13] is the only species that may not be present in either phase. Figure 1 displays the molecular structure of the most stable complex (**O**-complex) both in the gas phase and in THF. The enhanced thermodynamic stability of the **O**-complex can be seen in the following structural features: (1) The distance between Li and the ring oxygen is 2.082 Å and the O−Li···O3 angle is 104.7°, strongly indicating that the intramolecular Li coordination is as strong as the usual Li coordination at a C═C bond and that it may be achieved

(6) For recent reviews on this subject, see: (a) Romo, D.; Meyers, A. I. *Tetrahedron* **1991**, *47*, 9503. (b) Groaning, M. D.; Meyers, A. I. *Tetrahedron* **2000**, *56*, 9843. Papers relevant to this work: (c) Meyers, A. I.; Seefeld, M. A.; Lefker, B. A.; Blake, J. F.; Williard, P. G. *J. Am. Chem. Soc.* **1998**, *120*, 7429. (d) Lefker, B. A. Ph.D. Thesis, Colorado State University, 1988. (e) Thottathill, J. K.; Maniot, J. L.; Mueller, R. H.; Wong, M. K. Y.; Kissik, T. P. *J. Org. Chem.*, **1986**, *51*, 3140.

(7) Ikuta, Y.; Tomoda, S. *Tetraheron Lett.* **2003**, *44*, 5931.

(8) Meyers, A. I.; Seefeld, M. A.; Lefker, B. A.; Blake, J. F. *J. Am. Chem. Soc.* **1997**, *119*, 4565 and references therein.

(9) All computations were performed with *Gaussian 98*, Rev. A.7 (Frisch, M. J.; Trucks, G. W.; Schlegel, H. B.; Scuseria, G. E.; Robb, M. A.; Cheeseman, J. R.; Zakrzewski, V. G.; Montgomery, J. A., Jr.; Stratmann, R. E.; Burant, J. C.; Dapprich, S.; Millam, J. M.; Daniels, A. D.; Kudin, K. N.; Strain, M. C.; Farkas, O.; Tomasi, J.; Barone, V.; Cossi, M.; Cammi, R.; Mennucci, B.; Pomelli, C.; Adamo, C.; Clifford, S.; Ochterski, J.; Petersson, G. A.; Ayala, P. Y.; Cui, Q.; Morokuma, K.; Malick, D. K.; Rabuck, A. D.; Raghavachari, K.; Foresman, J. B.; Cioslowski, J.; Ortiz, J. V.; Baboul, A. G.; Stefanov, B. B.; Liu, G.; Liashenko, A.; Piskorz, P.; Komaromi, I.; Gomperts, R.; Martin, R. L.; Fox, D. J.; Keith, T.; Al-Laham, M. A.; Peng, C. Y.; Nanayakkara, A.; Gonzalez, C.; Challacombe, M.; Gill, P. M. W.; Johnson, B.; Chen, W.; Wong, M. W.; Andres, J. L.; Gonzalez, C.; Head-Gordon, M.; Replogle, E. S.; Pople, J. A. Gaussian, Inc.: Pittsburgh, PA, 1998) at the B3LYP level using 6-31G(d) basis for all optimizations except for Br, for which Huzinaga basis[10] with polarization (43321/4321/321*) was used. Solvent effects were calculated in tetrahydrofuran (THF) (dielectric constant = 7.52) using Tomasi's PCM and the CPCM method[11] at the B3LYP/6-311+G(d,p) level using the same Huzinaga basis for Br.

(10) Huzinaga, S. *Gaussian Basis Sets for Molecular Calculations;* Elsevier: Amsterdam, 1984.

(11) Barone, V., Cossi, M. *J. Phys. Chem. A* **1998**, *102*, 1995.

(12) Nomenclature of monomer enolate **2**: **C**-*endo* and **C**-*exo* = the intramolecular Li−$\pi_{C=C}$ complexes (Li coordinates the π-bond from the *endo*- and *exo*-faces, respectively), **N** = the intramolecular Li−N complex, **F** = the free Li enolate, and **O** = intramolecular Li−O complex.[7] It should be mentioned that analogous intramolecular complex of **1** could not be found after repeated attempts of geometry optimization using the same method, presumably because of severe skeletal strain if it were formed.

(13) Previous study[7] has shown that Li coordination at the enolate C═C bond causes significant pyramidalization at C7 (α-carbon) owing to the presence of the amide nitrogen atom. Such pyramidalization occurs away from the Li, causing significant steric relaxation as well as HOMO expanse over the Li-face (EFOE analysis), which allows preferential alkyl halide attack from the Li-face. According to the results of EFOE analysis[14] of **C**-*exo* species from **2** (EFOE densities (%) and PDAS values (au^3) at C7: *exo*-face, 1.425%, 51.7 au^3 and *endo*-face, 0.889%, 18.6 au^3), it is highly likely that it should undergo nearly exclusive *exo*-alkylation.

Figure 1. Structure of the most stable complex of Meyers-type enolate **2**. (B3LYP/6-31G(d); bond lengths are in angstroms and angles in degrees).

without much steric strain. (2) The nonbonded Li···C8 distance is short (2.043 Å), but the Li does not interact with C7 any more (Li···C7 = 2.569 Å; total of the three bond angles around C7 is 358.2°). (3) The enolate moiety remains coplanar (total of the three bond angles around C8 is 358.5°). It is strongly suggested that the tricyclic skeleton must be quite rigid without much steric strain.

Contrary to our expectation, however, an analysis based on the exterior frontier orbital extension model (the EFOE model)[14] showed that the major enolate (the **O**-complex) should not undergo exclusive *exo*-alkylation. Although the *exo*-face of the C=C bond at C7(α) (PDAS = 77.8 au^3) is indeed much less sterically hindered than the *endo*-face (35.3 au^3), the π-facial difference in HOMO extension is marginal but shows slight *endo* preference (EFOE density; 1.123% (*endo*-face), 0.945% (*exo*-face)). Apparently the EFOE model fails to predict exclusive *exo*-attack, unlike the previous case of enolate **3**.[7] Ground-state factors may not be responsible for the remarkable stereochemical reversal of **2**.

To this end, transition states (TS) for the alkylation of **2** were located at the B3LYP/6-31G(d) level using MeBr as an alkylating agent.[9−11] Figure 2 and Table 2 show five TS structures (**A**−**E**) and their relative populations at 195.15 K (−78 °C) calculated from the electronic energies with ZPE correction assuming the Boltzmann distribution. Each TS had a single imaginary vibrational mode corresponding to the stretching vibration of the forming bond (C7···CBr).[15] TS structures **A**, **C**, and **D** represent *endo* stereochemical processes. They are presumed to be derived from enolate species **C**-, **N**-, and **O**-complexes (Figure 1), respectively. On the other hand, TS structures **B** and **E** show *exo*-stereochemistry and may be derived from **C**- (or **N**-)[16] and

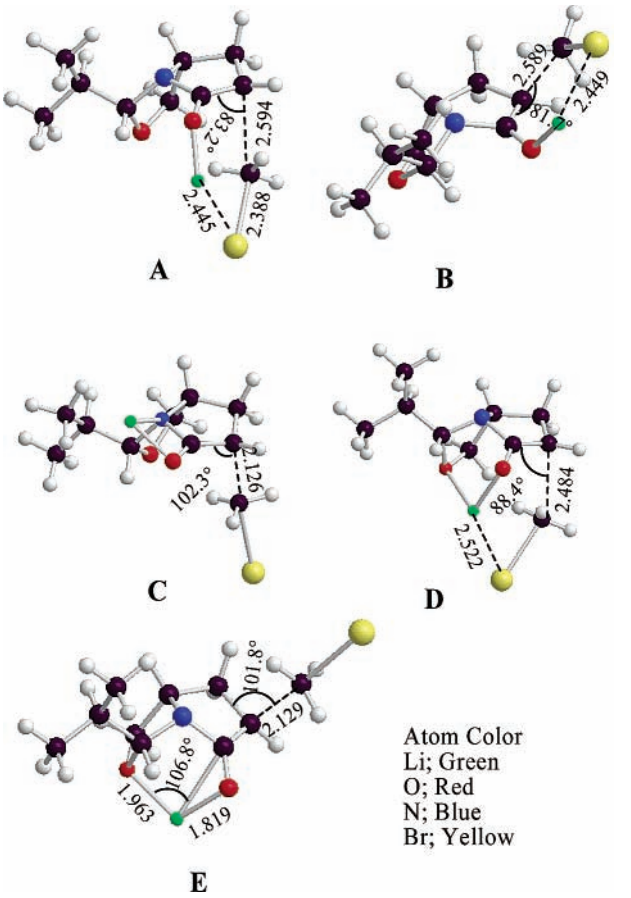

Figure 2. Transition structures for the reaction of enolate (**2**) with MeBr in the gas phase. (B3LYP/6-31G(d); bond lengths are in angstroms and angles in degrees).

O-complexes, respectively. The three TS structures **A**, **B**, and **D** show the interaction between Li and Br: the nonbonded Li···Br distances (2.445, 2.449, and 2.522 Å, respectively) are far shorter than the sum of their van der

Table 2. Calculated Stereoselectivity of the Alkylation of **2** with MeBr[a]

TS[b]	stereo-chemistry	gas phase (%)[c]	THF (%)[c,d] B3LYP	THF (%)[c,d] MP2	μ (D)[e]
A (**C**-*endo*)	*endo*	68.6	4.4	0.9	2.4
B (**C**-*exo*)	*exo*	31.4	0.5	4.1	1.4
C (**N**)	*endo*	0.0	0.0	0.6	17.4
D (**O**)	*endo*	0.0	0.0	0.0	5.2
E (**O**)	*exo*	0.0	95.0	94.5	17.5
exo: *endo* ratio		69:31	96:4	99:1	

[a] The transition states (TS, Figure 2) were located at the B3LYP/6-31G(d) level[9] with Huzinaga basis sets for Br.[10] [b] Refer to Figure 2 for TS notations and structures. The enolate notations indicated in parentheses are those from which the TS is presumed to be derived. [c] Process ratios of TSs were calculated assuming the Boltzmann distribution at −78 °C. [d] THF = tetrahydrofuran. 6-311+G(d,p) basis was employed for both B3LYP and MP2 calculations using the CPCM method implemented in Gaussian 98.[9,11] [e] μ = calculated dipole moment of TS in debyes.

(14) The EFOE (exterior frontier orbital electron) model[2b] assumes that FMO extension and reagent accessible space (steric effects; π-plane-divided accessible space = PDAS value) outside the molecular surface (van der Waals surface) of the reactant should be major factors of facial stereoselection. EFOE analysis was performed at the HF/6-31G(d) level with a lattice mesh of 0.1 au. Molecular surface was defined by Bondi's van der Waals radii. Integration of EFOE density was performed up to 10 au from the van der Waals surface. PDAS integration was performed up to 5 au from the van der Waals surface.

(15) The imaginary stretching vibrations for transition states **A**, **B**, **C**, **D** and **E** are −353.7, −364.4, −488.0, −430.4, and −508.3 cm^{-1}, respectively.

(16) The *exo*-TS starting from the **N**-complex converged into the *exo*-TS from **C**-complex (TS **A**).

Waals radii (3.67 Å). The incipient bond lengths and the approach angles of these TSs are 2.4−2.6 Å and 82−88°. In sharp contrast, the remaining TS structures (**C** and **E**), in which nonbonded interaction between Li and Br is not observed, show shorter incipient bond lengths (2.126 and 2.129 Å) and larger reagent approach angles (102.3° and 101.8°).

Table 2 shows the Boltzmann distribution of TS both in the gas phase and in THF solution at the experimental temperature (−78 °C). In the gas phase, the transition states **A** and **B** may proceed (68.6% and 31.4%, respectively), but the other TSs (**C**, **D**, and **E**) may not proceed (0.0%). The major pathway **A** (68.6%), which must be derived from the *endo*-attack of MeBr at C7 of the **C**-*endo* complex, is the *endo*-process. The total *exo*:*endo* ratio (31:69) is inconsistent with observed stereoselectivity (*exo*:*endo* = 99:1). To our surprise, the calculated stereochemistry is reversed in THF solution. Process **A**, the major one in the gas phase, almost vanishes in THF (0.9−4.4%). Instead, the *exo*-process **E**, which might also be derived from the **O**-complex, becomes a major pathway (∼95%) and process **C**, which is zero in the gas phase, shows up (0.6% at the MP2 level) in THF: the total *exo*:*endo* ratio is 99:1 at the MP2/6-311+G(d,p) level, in complete agreement with experiment. Importance of solvent effects on π-facial diastereoselection may be emphasized in the alkylation of Meyers-type enolates with alkyl halides as a typical bimolecular nucleophilic substitution reaction (S_N2). It should be noted here that in transition state **E**, the dihedral angle between the incipient bond and the adjacent antiperiplanar bond (C6−H_{endo}) is 128°, indicating limited importance of antiperiplanar hyperconjugative stabilization effects in this most probable TS.

The dramatic changes in stereoselectivity from gas phase to solution may be rationalized as follows. As shown in the last column of Table 2, *exo*-process **E**, a major path in THF, has a considerably high dipole moment (μ = 17.5 D), presumably because the charges are far apart ($Li^{+\delta}\cdots Br^{-\delta}$ distance is 7.431 Å), and the TS should be highly susceptible to the electrostatic field of solvent.

In summary, we have shown that the origin of stereochemical reversal between oxazolidine lactam enolates **1** and **2** would be the intervention of the stable enolate of **2**, in which Li interacts strongly with the ring oxygen atom within the concave of the bicyclic system (the **O**-complex; Figure 1). Owing to the highly polarized nature in the transition state of the *exo*-alkylation process with MeBr (transition state **E**; Figure 2), the process would be effectively stabilized by the electrostatic field of THF solvent.

Acknowledgment. We thank Japan Society for the Promotion of Science for financial support through a Grand in Aid for Scientific Research (09440215).

Supporting Information Available: Description of Cartesian coordinates and computational data of all structures. This material is available free of charge via the Internet at http://pubs.acs.org.

OL036021Q